**AOL – Spring 2014**

# Wavefront Sensing

The Shack Hartmann Wavefront Sensor system provides accurate, high-speed measurements of the wavefront shape and intensity distribution of beams by analyzing the location and intensity of spots (spotfield) formed by imaging a beam of light onto a CCD camera with a microlens array. These wavefront sensors can dynamically optimize the wavefronts of laser sources, characterize the wavefront distortion caused by optical components, and provide real-time feedback for the control of adaptive optics.

## Principle of operation

The Shack-Hartmann wavefront sensor uses a microlens array in conjunction with a CCD array. A planar wavefront that is transmitted through a microlens array and imaged on a CCD sensor will form a regular pattern of bright spots. If, however, the wavefront is distorted, the light imaged on the CCD sensor will consist of some regularly spaced spots mixed with displaced spots and missing spots. This information is used to calculate the shape of the wavefront that was incident on the microlens array. Shack-Hartmann type wavefront sensors can be used to characterize the performance of optical systems. In addition, they are increasingly used in applications where real-time monitoring of the wavefront is used to control an adaptive optic with the intent of removing the wavefront distortion before creating an image.

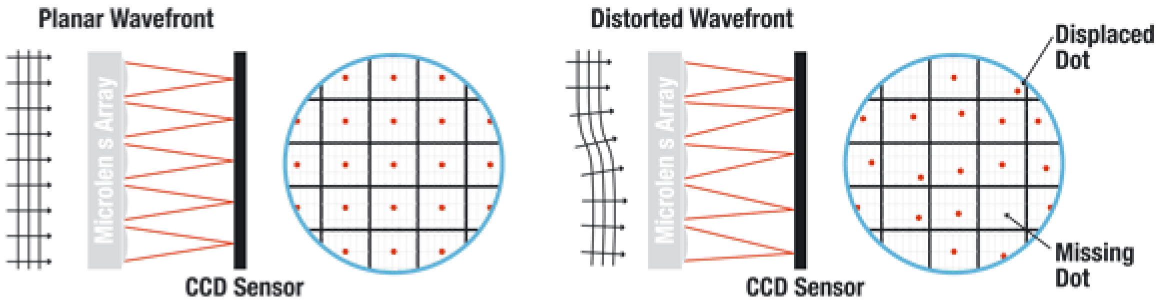


Figure 1: Principle of operation of the Shack-Hartmann wavefront sensor

## Wavefront Distortion and Spot Displacement

Each microlens of the lenslet array collects the light falling onto its aperture and generates a single spot on the detector plane (CCD camera) that is situated a focal length behind the lenslets. The spot positions are straight behind the lenses (green) only in case the launched wavefront is flat and parallel to the plane of the lenslets. We call these the Reference Spot Positions or reference spotfield. In the common case however, the current spot positions will be deviated in X and Y direction (red), that is, every spot lies away from the optical axis z of its associated microlens, separated by an angle α. It can be easily shown that this is caused by an incoming wavefront with the same average angle α compared to the reference wavefront.

$$\tan \alpha = \frac{\Delta z}{\Delta y} = \frac{\delta y}{f_{ML}}$$

When W($x$,$y$) describes the shape of the wavefront so its partial derivation relative to $x$ and $y$ are determined by the spot shift $\delta x$ and $\delta y$, respectively as well as by the distance between microlens and detector which is usually the focal length of the microlens $f_{ML}$

$$\frac{\partial}{\partial x} W(x,y) = \frac{\delta x}{f_{ML}} \qquad \frac{\partial}{\partial y} W(x,y) = \frac{\delta y}{f_{ML}} \tag{1}$$

The spot deviations $\delta x$ and $\delta y$ are determined by calculating the centroid coordinates of all detectable spots and subtracting the corresponding reference coordinates. These spot deviations are integrated within a two-dimensional integration process that gives the wavefront W(*x*,*y*).

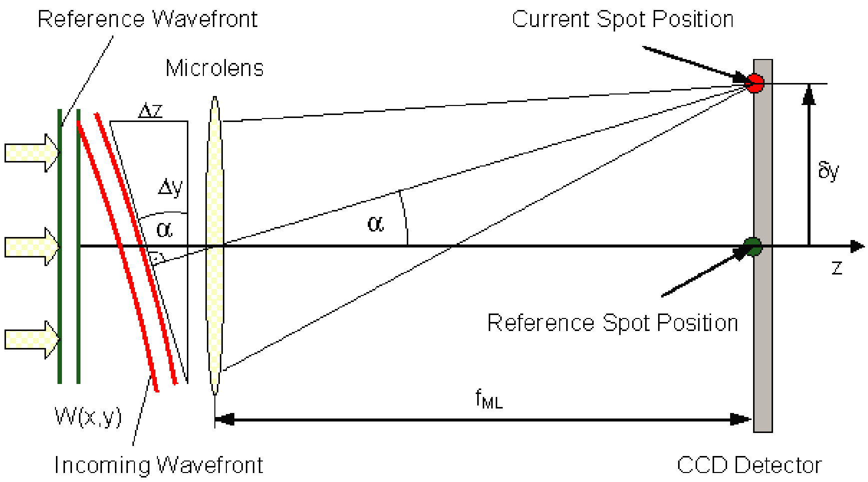


Figure 2: Diagram for calculating wavefront aberrations

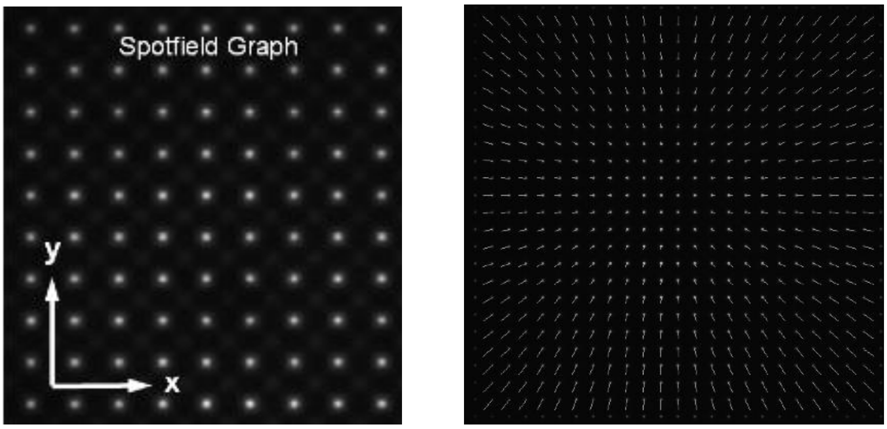


Figure 3: Spot field as obtained from the CCD camera (Left ). Spot Shifts displayed as short lines between the actual spot (centroid) position and its corresponding reference position.

**Zernike polynomials and wavefront aberrations**

Optical system aberrations have traditionally been described by power series expansions. Many optical systems have circular pupils and the experimental application typically requires data fitting. Hence, it is desirable to expand the wave aberrations in terms of a complete set of basis functions that are orthogonal over the interior of a circle.

There is an increasing interest in correcting higher order aberrations of optical systems such as telescopes or the eye. For example, in vision only defocus and astigmatism are currently being corrected but there is potential to improve vision well beyond 20/20. This is of interest in eye laser surgery and imaging of the retina using adaptive optics.

While defocus and astigmatism can be determined using a set of lenses, higher order corrections require precise measurement of optical aberrations and more sophisticated techniques. Such techniques include interferometry and Shack-Hartmann wavefront sensors.

A mathematical description of aberrations, such as expansions in Zernike polynomials, is required to provide an accurate description and estimation of the wave aberration function. Zernike polynomials are made up of terms that are of the same form as the types of aberrations often observed in optical tests. Zernike polynomials are widely used for describing wave aberration functions and for data fitting of experimental measurements. However, they are only one of an infinite number of complete sets of polynomials that are orthogonal over the interior of a unit circle

**Wavefront aberration**

In an imaging system, the wavefront aberration, W(*x*,*y*), is the distance, in optical path length, from the reference sphere (corresponding to a diffraction limited system) to the actual wavefront in the exit pupil measured along the ray as a function of the transverse coordinates (*x*,*y*) of the ray intersection with the reference sphere. The wavefront aberration is the departure of the exit pupil wavefront from the reference sphere. The relation between the wavefront aberration function and the point spread function of an imaging system is given by

$$h(x,y) \propto FT\left\{ p(x,y)\exp\left[ -j\frac{2\pi}{\lambda}W(x,y) \right] \right\} \Bigg|_{f_x=\frac{x}{\lambda z_i},\, f_y=\frac{y}{\lambda z_i}}$$

where *p(x,y)* represents the exit pupil and $z_i$ the distance from the exit pupil to the image plane [1].

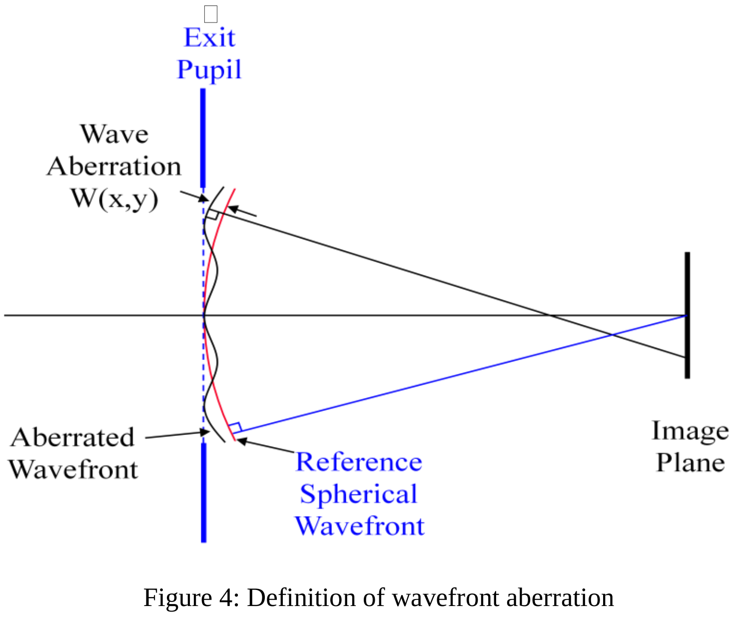


Figure 4: Definition of wavefront aberration

The Zernike polynomials form a complete set of functions that are orthogonal over a circle of unit radius. They can be expressed in polar or Cartesian coordinates and are scaled so that all modes (other than the zero order) have zero mean and unit variance. Accordingly, wave aberrations in an optical system with a circular pupil are described by a weighted sum of Zernike polynomials, where each coefficient corresponds to the RMS contribution of each mode.

The Zernike polynomials are defined as follows

$$Z_n^m(\rho,\theta) = \begin{cases} N_n^m R_n^{|m|}(\rho)\cos(m\theta) & \text{for } m \ge 0\,,\quad 0 \le \rho \le 1\,,\quad 0 \le \theta \le 2\pi \\ -N_n^m R_n^{|m|}(\rho)\sin(m\theta) & \text{for } m < 0\,,\quad 0 \le \rho \le 1\,,\quad 0 \le \theta \le 2\pi \end{cases}$$

Given *n, m* can only take values $-n, -n+2, -n+4, \ldots, n$

The normalization factor is $N_n^m = \sqrt{\dfrac{2(n+1)}{1+\delta_{m0}}}$ $\quad \delta_{m0} = 1$ for $m = 0$, $\quad \delta_{m0} = 0$ for $m \ne 0$

The radial polynomials are $R_n^{|m|}(\rho) = \displaystyle\sum_{s=0}^{(n-|m|)/2} \frac{(-1)^s (n-s)!}{s!\,[0.5(n+|m|)-s]!\,[0.5(n-|m|)-s]!}\,\rho^{n-2s}$

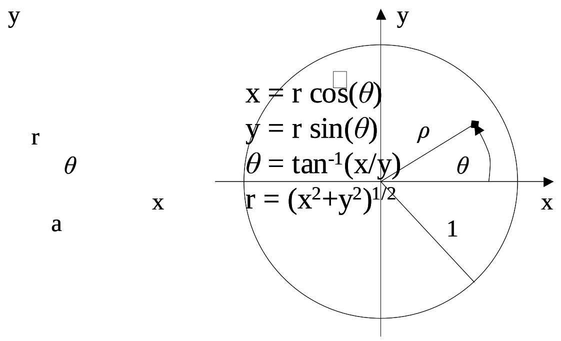


x = $\rho$ cos($\theta$)
y = $\rho$ sin($\theta$)
$\theta$ = tan$^{-1}$(x/y)
$\rho$ = r/a = (x$^2$+y$^2$)$^{1/2}$

Fig. 5: Normalized pupil coordinates for a circular pupil of radius a.

The wave aberrations are expressed as a sum of Zernike polynomials in either polar or Cartesian coordinates:

$$W(\rho,\theta) = \sum_n^k \sum_{m=-n}^{n} W_n^m Z_n^m(\rho,\theta) \quad ; \quad W(x,y) = \sum_{j=0}^{j\,\max} W_j Z_j(x,y)$$

| order $n$ | frequency $m$ | $Z_n^m(\rho,\theta)$ | Meaning |
|---|---|---|---|
| 0 | 0 | $1$ | Constant term, or Piston |
| 1 | -1 | $2\rho\sin(\theta)$ | Tilt in y - direction, Distortion |
| 1 | 1 | $2\rho\cos(\theta)$ | Tilt in x - direction, Distortion |
| 2 | -2 | $\sqrt{6}\rho^2\sin(2\theta)$ | Astigmatism with axis at $\pm 45^\circ$ |
| 2 | 0 | $\sqrt{3}(2\rho^2-1)$ | Field curvature, Defocus |
| 2 | 2 | $\sqrt{6}\rho^2\cos(2\theta)$ | Astigmatism with axis at $0^\circ$ or $90^\circ$ |
| 3 | -3 | $\sqrt{8}\rho^3\sin(3\theta)$ | |
| 3 | -1 | $\sqrt{8}(3\rho^3-2\rho)\sin(\theta)$ | Coma along y - axis |
| 3 | 1 | $\sqrt{8}(3\rho^3-2\rho)\cos(\theta)$ | Coma along x - axis |
| 3 | 3 | $\sqrt{8}\rho^3\cos(3\theta)$ | |
| 4 | -4 | $\sqrt{10}\rho^4\sin(4\theta)$ | |
| 4 | -2 | $\sqrt{10}(4\rho^4-3\rho^2)\sin(2\theta)$ | Secondary Astigmatism |
| 4 | 0 | $\sqrt{5}(6\rho^4-6\rho^2+1)$ | Spherical Aberration, Defocus |
| 4 | 2 | $\sqrt{10}(4\rho^4-3\rho^2)\cos(2\theta)$ | Secondary Astigmatism |
| 4 | 4 | $\sqrt{10}\rho^4\cos(4\theta)$ | |
| ⋮ | ⋮ | ⋮ | |

**Table I:** List of 14 Zernike polynomials

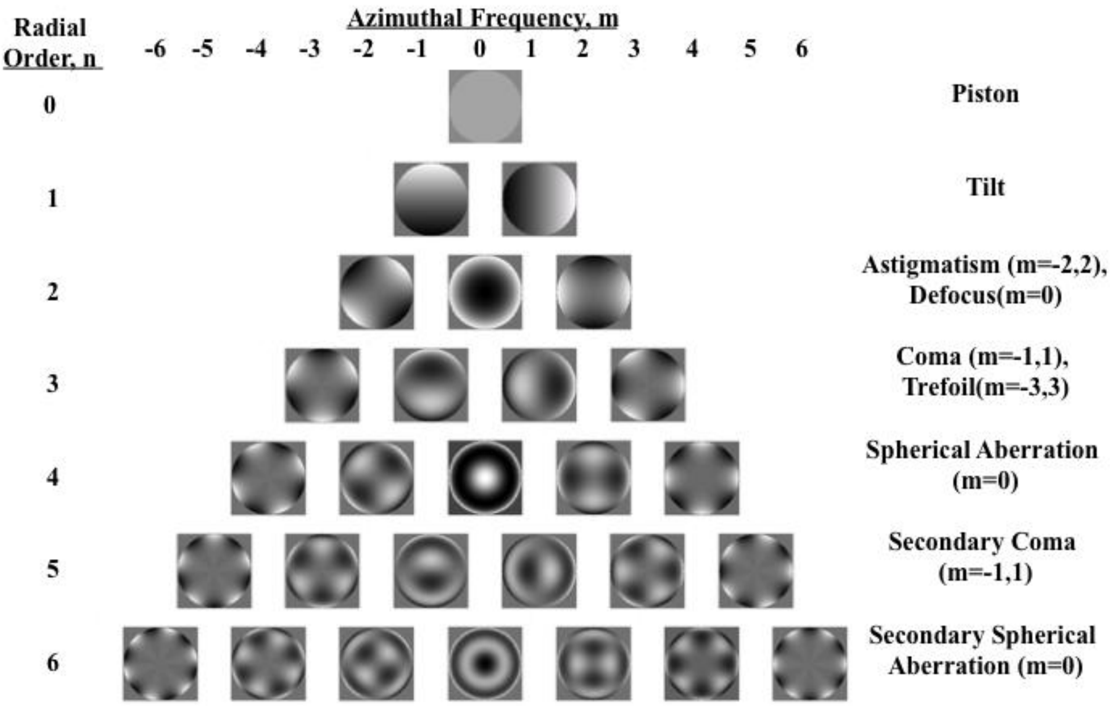


**Table II:** Graphic representation of Zernike polynomials (first six orders) and common names

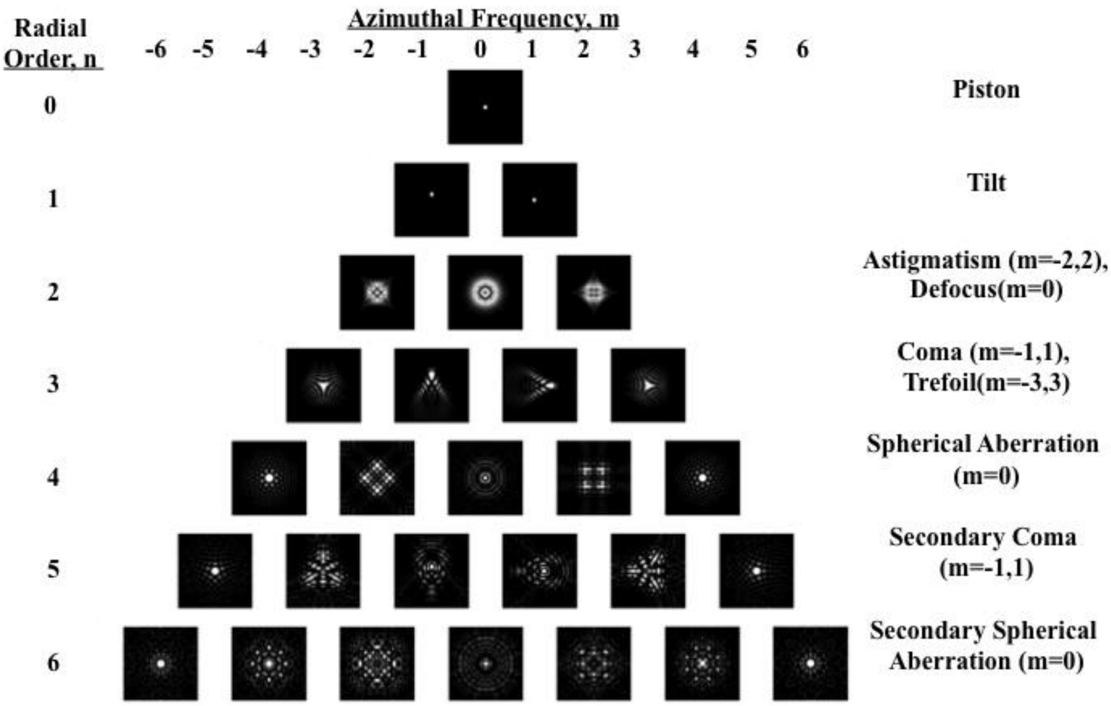


**Table III:** Point spread function of Zernike polynomials (of first six orders)

**Modal numbering schemes**

The natural scheme for ordering of the Zernike modes is to use a double index corresponding to the radial order and angular frequency as shown above. However, for numerical purposes it is useful to have a single-index scheme, which allows the Zernike coefficients to be written as a vector for use in linear algebra calculations. Numerous schemes for ordering the Zernike modes have been proposed in the optics literature, each with its own advantages and disadvantages. The Malacara scheme illustrated in Table V has the distinct advantage of corresponding to the order of generation of the various modes by his automatic generating function given by

r = n(n+1)/2 + (n-m)/2 +1 .

Malacara's generating function is of great practical value because Zernike modes of higher order have many algebraic terms, which increases the likelihood of inadvertent errors when entering the analytical formulas into a computer. These potential errors are eliminated when a computer algorithm generates the symbolic expressions.

| Mode | Order | Freq | Norm | Zernike polynomial |
|---|---|---|---|---|
| 1 | 0 | 0 | 1 | 1 |
| 2 | 1 | 1 | 2 | r*sin(θ) |
| 3 | 1 | -1 | 2 | r*cos(θ) |
| 4 | 2 | 2 | √6 | $r^2$*sin(2θ) |
| 5 | 2 | 0 | √3 | $2r^2$ -1 |
| 6 | 2 | -2 | √6 | $r^2$*cos(2θ) |
| 7 | 3 | 3 | 2√2 | $r^3$*sin(3θ) |
| 8 | 3 | 1 | 2√2 | $3r^3$*sin(θ) -2r*sin(θ) |
| 9 | 3 | -1 | 2√2 | $3r^3$*cos(θ) -2r*cos(θ) |
| 10 | 3 | -3 | 2√2 | $r^3$*cos(3θ) |
| 11 | 4 | 4 | √10 | $r^4$*sin(4θ) |
| 12 | 4 | 2 | √10 | $4r^4$*sin(2θ) -$3r^2$*sin(2θ) |
| 13 | 4 | 0 | √5 | $6r^4$ -$6r^2$ +1 |
| 14 | 4 | -2 | √10 | $4r^4$*cos(2θ) -$3r^2$*cos(2θ) |
| 15 | 4 | -4 | √10 | $r^4$cos(4θ) |

Table IV: Malacara's mode ordering

**Wavefront aberration data fitting with Zernike polynomials**

The goal is to express the wavefront aberrations as a superposition of Zernike polynomials $Z_j$

$$W(x,y) = \sum_j W_j Z_j(x,y)$$

where $W_j$ are the coefficients of the $Z_j$ mode expansion. In other words, $W_j$ is the rms wavefront error for the mode $Z_j$.

Taking derivatives on both sides of the equation with respect to *x* and *y* we obtain

$$\frac{\partial W(x,y)}{\partial x} = \sum_j W_j \frac{\partial Z_j(x,y)}{\partial x} \quad ; \quad \frac{\partial W(x,y)}{\partial y} = \sum_j W_j \frac{\partial Z_j(x,y)}{\partial y}$$

and using Eq. 1

$$\frac{\delta x(x,y)}{f_{ML}} = \sum_j W_j \frac{\partial Z_j(x,y)}{\partial x} \quad ; \quad \frac{\delta y(x,y)}{f_{ML}} = \sum_j W_j \frac{\partial Z_j(x,y)}{\partial y} \qquad (2)$$

The Eqs. (2) are then used to calculate $W_j$ using least-squares estimation. For this purpose, the equations are written in matrix form. For brevity we call the measured data

$$\frac{\delta x(x,y)}{f_{ML}} = p(x,y) \quad \text{and} \quad \frac{\delta y(x,y)}{f_{ML}} = q(x,y)$$

and the polynomial derivatives, which need to be determined only once,

$$\frac{\partial Z_j(x,y)}{\partial x} = Z^x{}_j(x,y) \quad \text{and} \quad \frac{\partial Z_j(x,y)}{\partial y} = Z^y{}_j(x,y).$$

In matrix form, Eq. (2) is

$$\begin{bmatrix} p(x_1,y_1) \\ p(x_1,y_2) \\ \vdots \\ p(x_k,y_k) \\ q(x_1,y_1) \\ q(x_1,y_2) \\ \vdots \\ q(x_k,y_k) \end{bmatrix} = \begin{bmatrix} Z^x{}_1(x_1,y_1) & Z^x{}_2(x_1,y_1) & \cdots & Z^x{}_M(x_1,y_1) \\ Z^x{}_1(x_1,y_2) & Z^x{}_2(x_1,y_2) & \cdots & Z^x{}_M(x_1,y_2) \\ \vdots & \vdots & \cdots & \vdots \\ Z^x{}_1(x_k,y_k) & Z^x{}_2(x_k,y_k) & \cdots & Z^x{}_M(x_k,y_k) \\ Z^y{}_1(x_1,y_1) & Z^y{}_2(x_1,y_1) & \cdots & Z^y{}_M(x_1,y_1) \\ Z^y{}_1(x_1,y_2) & Z^y{}_2(x_1,y_2) & \cdots & Z^y{}_M(x_1,y_2) \\ \vdots & \vdots & \cdots & \vdots \\ Z^y{}_1(x_k,y_k) & Z^y{}_2(x_k,y_k) & \cdots & Z^y{}_M(x_k,y_k) \end{bmatrix} \begin{bmatrix} W_1 \\ W_2 \\ \vdots \\ W_M \end{bmatrix}$$

where the coordinates $(x_k, y_k)$ correspond to the coordinates of each microlens in the Shack-Hartmann sensor. In shorthand notation

$$\mathbf{B} = \mathbf{AW}$$

The least squares estimate of $\mathbf{W}$ is

$$\mathbf{W}_{\mathrm{LS}} = (\mathbf{A}^T\mathbf{A})^{-1}\mathbf{A}^T\mathbf{B} \qquad (3)$$

with $\mathbf{A}^T$ the transpose of $\mathbf{A}$.

The $Z^x{}_j(x,y)$ and $Z^y{}_j(x,y)$ are orthogonal because the $Z_j(x,y)$ are orthogonal. Hence, the columns of $\mathbf{A}$ are orthogonal and $\mathbf{A}^T\mathbf{A}$ is diagonal. Therefore, Eq. (3) states that the wavefront aberration coefficients are obtained by projection of the data onto the partial derivatives of the Zernike polynomials ( $\mathbf{A}^T\mathbf{B}$) and multiplication by a diagonal matrix $\mathbf{A}^T\mathbf{A}$.

**References**

[1] Joseph W. Goodman, Introduction to Fourier Optics, Roberts & Company, Colorado, 2005.
[2] D. Malacara, Optical Shop Testing, 2nd ed., John Wiley & Sons, Inc., New York, 1992.
[3] www.thorlabs.com
[4] V. N. Mahajan, Optical Imaging and Aberrations, Part I Ray Geometrical Optics, SPIE Press, 1998.